



and significantly uplifted by Moth-Poulsen and co-workers with their several experimental and theoretical studies. These investigations have inspired the scientific research community to further inspect the chemical photoswitches for MOST applications.<sup>5,17–19,21,22,27–35</sup> Hitherto, a variety of molecular photoswitches, including the tetracarbonyl-fulvalene-diruthenium complexes, anthracenes, norbornadiene/quadracyclane (NBD/QC), dihydroazulene/vinylheptafulvene, azobenzenes, *etc.*, are known.<sup>5,21,29,32,33,36–55</sup> Among all, the NBD/QC couple, which involves the [2+2]-cycloaddition of bridged bicyclodiene molecule to give a strained metastable photoadduct is extensively investigated for MOST applications due to its high energy storage density.<sup>5,22,31,41,54–56</sup> However, the low thermal back-reaction barrier and optical absorption in the UV region hinders its practical applicability as an effective MOST systems.<sup>16–18</sup> *En route* to make NBD/QC couple relevant for the practical real-life application, research has also been conducted to tune their thermochemical and photophysical properties *via* different substitutions.<sup>5,14,21,26,57</sup> Despite of enormous efforts, a photoswitching couple with all the desired properties for practical MOST applications has not been achieved yet.<sup>5,14</sup> This is because incorporating all the essential features in a single photochromic couple for their practical MOST application is extremely challenging.<sup>5,21,24</sup>

Recently, the Moth-Poulsen and Mikkelsen groups demonstrated that an increase by one methylene ( $-\text{CH}_2-$ ) bridging unit in the NBD/QC system results in a bicyclooctadiene/tetracyclooctane (BOD/TCO) couple with an enhanced storage energy.<sup>17,18</sup> Thereafter, a high-throughput screening of nearly half a million photoswitches carried out to analyse the MOST applications reveals that the best properties were mostly exhibited by the systems with longer bridges.<sup>58</sup> Further increases in bridge length of the bicyclic diene improves the storage energy but compromises the thermal back reaction (TBR) barrier.<sup>16</sup> This is attributed to ring strain, however the strain energy has not been quantitatively assessed, which is certainly crucial for rational designing of the photoswitching systems in the future. More recently, the influence of *N*-substitution on the properties of a BOD/TCO photoswitch has been reported, however there is no clue for the effect of *N*-substitution with the different bridge lengths.<sup>59</sup>

In the present investigation, ring strain in various bicyclic diene photoswitching systems with different bridge lengths were quantified. Further, the impacts of ring strain on the thermochemical properties are discussed to assist future MOST system designing and engineering. The prominent objective is to forecast the influence of the position of aza-substitution on the thermochemical and photophysical properties of various bicyclic diene photoswitching systems with different bridge lengths.

## 2. Computational details

The geometries of all the reactants, transition states (TS) and products were fully optimized employing the M06-2X functional and 6-311++G\*\* Pople-style basis set without any geometrical or

symmetrical constraints. Previous benchmarking studies of both the NBD/QC and BOD/TCO photoswitching couples suggest that the geometry and thermochemical properties are better predicted with the M062X/6-311++G\*\* level of theory.<sup>17,55</sup> Therefore, the same method was employed for the computation of the studied bicyclodiene photoswitches. The nature of the critical point structures was characterized as local minima by the harmonic frequency calculations. The time-dependent density functional theory (TD-DFT) calculations were performed to shed light on the photophysical properties of the photoswitching systems. The vertical excitation energies for first fifteen singlet electronic excited states were calculated with the TD-M06-2X/6-311++G\*\* method. The ring strain energy (SE) which is calculated as the difference between the energy of the molecule with the sum of the energy of the group equivalents in the molecule. SE is calculated at the M06-2X/6-31+G(2df,p) level of theory, as illustrated in a recent report.<sup>60</sup> All these calculations were performed using the Gaussian16 suite program.<sup>61</sup>

The harnessed solar energy that can be stored as chemical energy in a metastable photoproduct is the storage energy ( $\Delta G_{\text{str}}$ ) of the photoswitching couple. The storage energy is calculated as the difference between the Gibbs free energy of the metastable photoisomer and the parent molecule using the following equation:

$$\Delta G_{\text{str}} = G_{\text{photoproduct}} - G_{\text{parent}} \quad (1)$$

where  $G_{\text{parent}}$  and  $G_{\text{photoproduct}}$  are the Gibbs free energy of the parent molecule and the photoproduct, respectively. The difference in electronic energy ( $\Delta E_{\text{str}}$ ) and difference in thermal correction ( $\Delta G_{\text{thermal}}$ ) between the photoisomer and the parent molecules contributes to the total  $\Delta G_{\text{str}}$  as follows:

$$\Delta G_{\text{str}} = \Delta E_{\text{str}} - \Delta G_{\text{thermal}} \quad (2)$$

where  $\Delta E_{\text{str}}$  is the difference in electronic energy of the two photoisomers while  $\Delta G_{\text{thermal}}$  is the difference in the thermal energy contribution to the Gibbs free energy of the two photoisomers. To determine more accurate values, the storage energy was estimated by calculating the electronic energy ( $\Delta E_{\text{str}}$ ) at the DLPNO-CCSD(T)/Def2TZVP level using geometries optimized with M06-2X/6-311++G\*\*. Further, the thermal correction ( $\Delta G_{\text{thermal}}$ ) was included at the M06-2X/6-311++G\*\* level of theory, analogous to that in the previous report.<sup>16</sup>

The thermal back reaction barrier ( $\Delta G_{\text{TBR}}$ ) is the amount of activation energy required for back conversion of the metastable photoproduct into the parent isomer. It can be calculated as:

$$\Delta G_{\text{TBR}} = G_{\text{TS}} - G_{\text{photoproduct}} \quad (3)$$

where  $G_{\text{TS}}$  is the Gibbs free energy of the TS.

The transition state involves the formation of singlet biradicals during the thermal ring-opening of the metastable cycloadduct.<sup>22</sup> Owing to the multireference character of the transition state, the DFT functionals are inappropriate to predict the structure and often overestimates the thermal back reaction (TBR) barrier.<sup>22</sup> Previous benchmarking studies have revealed that the PBE functional is better to predict the





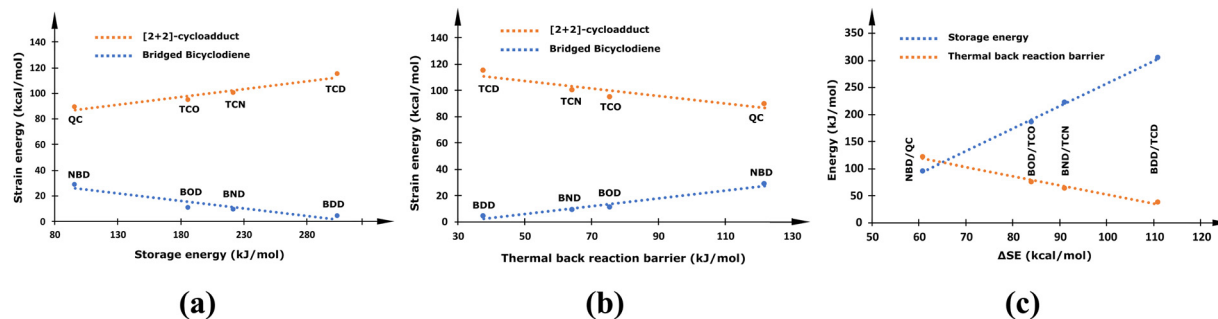


Fig. 1 Variation in thermochemical properties with molecular ring strain. (a) Variation in storage energy with the ring strain energy of the bridged bicyclodiene and photoproduct, (b) variation in the thermal back reaction with the ring strain energy of the bridged bicyclodiene and photoproduct, and (c) variation in thermochemical properties with the difference in ring strain energy between the bridged bicyclodiene and photoproduct ( $\Delta SE$ ).

the thermochemical properties with the ring SEs were analysed and the resulting data is systematically presented in Fig. 1. The calculated energy values are provided in S1 of the ESI† (Table S1).

The calculated ring strain energy decreases from 28.95 to 4.28 kcal mol<sup>-1</sup> with the progressive increase of  $-CH_2-$  units in the bridge (NBD to BDD) and the resulting bicyclic diene attains a high stability. However, the ring SE in the metastable [2+2]-cycloadduct obtained upon photoconversion increases from 89.75 to 115.19 kcal mol<sup>-1</sup> with bridge length (QC to TCD), thereby drastically increasing the instability of the photoproduct. Consequently, the difference in SE between the parent bicyclodiene and the corresponding cycloadduct ( $\Delta SE$ ) becomes larger (60.79 to 110.91 kcal mol<sup>-1</sup>) as the bridge length increases. Therefore, the storage energy is remarkably improved from the NBD/QC (96.06 kJ mol<sup>-1</sup>) to the BDD/TCD (304.39 kJ mol<sup>-1</sup>) photoswitching system. The enhanced instability induced due to ring strain in the metastable photoisomer upsurges its propensity to revert back to the parent molecule. Therefore, the barrier to a thermal back reaction decreases from 121.77 to 37.63 kJ mol<sup>-1</sup> with the increase in  $-CH_2-$  bridging units (QC to TCD). Overall, the ring strain energy of the photoisomers is crucial to modulate the thermochemical properties of the MOST applications, as can be clearly seen in Fig. 1. The increase in bridge length, although it enhances the storage energy, remarkably affects the storage time due to the enhanced ring strain in the metastable photoisomer. Therefore, a larger  $\Delta SE$  between two photoisomers can improve the thermochemical properties, provided that the ring strain in the metastable product does not increase significantly.

### 3.2 Thermochemical properties

**Storage energy ( $\Delta G_{str}$ ) and energy storage density.** Initially, the storage energy ( $\Delta G_{str}$ ) was determined for the various bicyclodiene-based photoswitches with different bridge lengths. The calculated  $\Delta G_{str}$  for the NBD/QC, BOD/TCO, BND/TCN, and BDD/TCD photoswitching couples is 96.06, 186.19, 222.00, and 304.39 kJ mol<sup>-1</sup> (Table S1). These values are obtained by computing the electronic energy with DLPNO-CCSD(T)/Def2TZVP and including the thermal correction at the M062X/6-311++G\*\* level for the geometries optimized with the M062X/6-311++G\*\* level of theory. In Table 1, the calculated storage energy and the first important excitation wavelength of the reactants and photoproducts are systematically compared with the previously reported data for bicyclic diene photoswitches. The calculated storage energy and the excitation wavelengths are in accordance with the previously reported values of 96.3 (NBD/QC), 192.8 (BOD/TCO), 223.0 (BND/TCN), and 305.8 (BDD/TCD) kJ mol<sup>-1</sup>. Further, the experimentally determined enthalpy for the isomerization of quadricyclane to norbornadiene is  $92.05 \pm 1.18$  kJ mol<sup>-1</sup> is also in agreement with the calculated data.<sup>64</sup> The norbornadiene shows the experimental absorption onset ( $\log \epsilon = 2$ ) at  $\sim 267$  nm in acetonitrile solvent, which is also closer to the excitation wavelength computed in the gaseous phase.<sup>65</sup> This ensures the reliability of the obtained outcomes.

*En route* to unravel the impact of *N*-substitution,  $\Delta G_{str}$  was estimated for the various *N*-substituted systems of different bicyclodiene photoswitches. The variation in  $\Delta G_{str}$  for different *N*-substitutions in the studied bicyclodiene systems with different bridge lengths is shown in Fig. 2. Herein, the  $\Delta G_{str}$  of parent molecular photoswitching systems was considered as

Table 1 Comparison of the calculated storage energy and first important excitation wavelength with previously reported data

System	Storage energy (kJ mol <sup>-1</sup> )		$\lambda_{reactant}$ (nm)		$\lambda_{product}$ (nm)	
	Calculated	Reported <sup>16</sup>	Calculated	Reported <sup>16</sup>	Calculated	Reported <sup>16</sup>
NBD/QC	96.06	96.30	214.42	213.65	184.63	190.74
BND/TCN	222.00	223.00	206.69	206.67	199.61	208.46
ABND/ATCN	220.32	220.50	242.09	250.44	207.27	223.07
OBND/OTCN	213.25	213.70	213.22	216.45	193.35	204.87
BDD/TCD	304.39	305.80	207.52	207.66	202.19	210.97
ABDD/ATCD	299.99	302.60	223.66	239.98	208.76	219.63
OBDD/OTCD	290.76	292.40	204.14	211.98	198.98	209.74



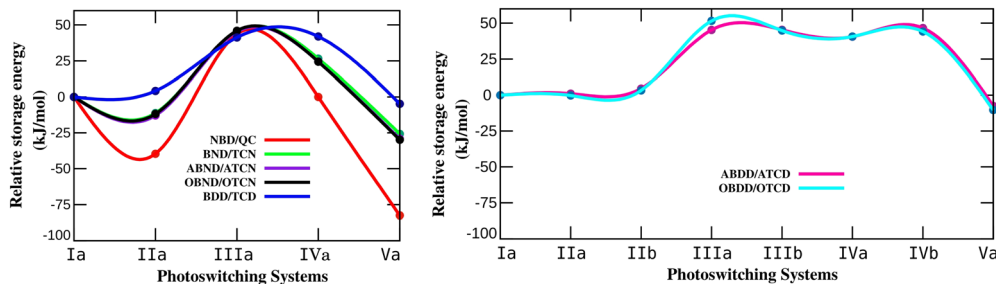


Fig. 2 Variation in the storage energy of *N*-substituted systems relative to their parent photoswitching system. The energy values were obtained by computing the electronic energy with the DLPNO-CCSD(T)/Def2TZVP method and including the thermal correction at the M062X/6-311++G\*\* level.

zero and the energies for different aza-substituted systems were accounted relative to their parent photoswitches. The calculated  $\Delta G_{\text{str}}$  values are provided in S2 of the ESI† (Tables S2–S8).

It has been observed that the presence of N at the bridgehead position (IIa-NBD/QC) decreases the storage energy to  $56.47 \text{ kJ mol}^{-1}$  when compared with that of the parent NBD/QC ( $96.06 \text{ kJ mol}^{-1}$ ) (Table S2 of the ESI†). The calculated storage energy for IIa-NBD/QC is in accordance with the previously reported value of  $53.81 \text{ kJ mol}^{-1}$  ( $12.86 \text{ kcal mol}^{-1}$ ) for the same system calculated with the B3LYP/6-311++G\* level.<sup>66</sup> The storage energy is significantly reduced to  $13.48 \text{ kJ mol}^{-1}$  in the Va-NBD/QC photoswitch, where both the bridgehead C atoms are replaced by N. Notably, the substitution of N at the unsaturated C of a bicyclodiene (IIIa-NBD/QC) significantly increases the storage energy up to  $139.77 \text{ kJ mol}^{-1}$ . This value is also in agreement with the earlier reported value of  $135.90 \text{ kJ mol}^{-1}$  ( $32.48 \text{ kcal mol}^{-1}$ ) for *N*-substitution at the unsaturated position in the NBD.<sup>66</sup> The storage energy of IVa-NBD/QC is  $96.02 \text{ kJ mol}^{-1}$  which is close to the parent NBD/QC system. This infers that the effect on  $\Delta G_{\text{str}}$  is only marginal if the bridgehead and closest unsaturated C of bicyclodiene are replaced by N. The observed trend of variation in storage energy with position of N in bicyclodiene-based photoswitches with different bridge lengths resembles that of the NBD/QC system and the recently reported BOD/TCO system.<sup>59</sup> This indicates that the position of N is crucial for modulating the storage energy in bicyclodiene-based photoswitches with different bridge lengths. Notably, the presence of N in the unsaturated position improves the storage energy, whereas replacing the bridgehead C with N may degrade the energy storage properties in the studied bicyclodiene based photoswitches.

Although the trend in  $\Delta G_{\text{str}}$  depends on the position of N, the extent of variation for the studied bicyclic dienes differs considerably with the bridge length. The reductions in  $\Delta G_{\text{str}}$  for the bridgehead *N*-substituted IIa- and Va-NBD/QC systems are  $39.59$  and  $82.58 \text{ kJ mol}^{-1}$ , respectively. A recently reported BOD/TCO couple displayed a decrease in  $\Delta G_{\text{str}}$  of  $19.42$  and  $39.12 \text{ kJ mol}^{-1}$  for the same bridgehead *N*-substituted systems.<sup>59</sup> However, the reductions in  $\Delta G_{\text{str}}$  in the BND/TCN, ABND/ATCN, and OBND/OTCN photoswitches are only  $11.24$  to  $12.90 \text{ kJ mol}^{-1}$  for the IIa and  $25.71$  to  $29.88 \text{ kJ mol}^{-1}$  for the Va systems.  $\Delta G_{\text{str}}$  is decreased by only  $0.23 \text{ kJ mol}^{-1}$  for the IIa-OBDD/OTCD couple. Interestingly, the  $\Delta G_{\text{str}}$  is even enhanced

by  $1.09$  to  $4.62 \text{ kJ mol}^{-1}$  in the IIa-BDD/TCD and IIa-ABDD/ATCD systems due to the presence of N at the bridgehead position. But, upon replacement of both bridgehead C atoms with N,  $4.76$  to  $10.39 \text{ kJ mol}^{-1}$  decreases in  $\Delta G_{\text{str}}$  of the Va-BDD/TCD, Va-ABDD/ATCD, Va-ABDD/ATCD systems are observed. The presence of a heteroatom (N or O) on the bridge has a comparatively minor effect on  $\Delta G_{\text{str}}$  of the bridged bicyclodiene-based photoswitches. These observations led to the inference that the reduction in  $\Delta G_{\text{str}}$  with *N*-substitution at the bridgehead position is more drastic for the NBD/QC system with short bridge lengths. Noteworthy, the decreasing effect in  $\Delta G_{\text{str}}$  becomes less prominent after elongation of the bridge with  $-\text{CH}_2-$  units. Therefore, the *N*-substitution at the bridgehead position provides better storage properties in bicyclodiene photoswitches with longer bridges.

It can be noted that the storage energy increases significantly when an unsaturated C is replaced with N in the studied bicyclodiene-based photoswitching systems. The enhancement in  $\Delta G_{\text{str}}$  is almost constant and ranges from  $41.26$  to  $51.59 \text{ kJ mol}^{-1}$  (Fig. 2) for the studied switches. This clearly suggest that, contrary to *N*-substitution at the bridgehead position, the increase in  $\Delta G_{\text{str}}$  of the photoswitching system due to unsaturated N in the bicyclic diene does not depend on the bridge length. Therefore, *N*-substitution at the unsaturated position of the bicyclodiene would be beneficial to improve the storage energy of all the studied bridged bicyclic diene switches.

Furthermore, there is no significant variation in  $\Delta G_{\text{str}}$  after replacement of the bridgehead and unsaturated C with N (IVa-NBD/QC) when compared with that of the parent NBD/QC system. According to a recent report,  $\Delta G_{\text{str}}$  in the BOD/TCO couple increases by  $14.34 \text{ kJ mol}^{-1}$  with N substitution at the bridgehead and unsaturated position. The increase in  $\Delta G_{\text{str}}$  is  $24.41$  to  $26.51 \text{ kJ mol}^{-1}$  for the IVa-BND/TCN, IVa-ABND/ATCN, and IVa-OBND/OTCN systems and  $40.59$  to  $46.66 \text{ kJ mol}^{-1}$  for the IVa-BDD/TCD, IVa-IVb-ABDD/ATCD, and IVa-IVb-OBDD/OTCD systems. This clearly indicates that substituting the bridgehead and unsaturated C with N tends to increase  $\Delta G_{\text{str}}$  with increasing bridge length of the bicyclodiene-based photoswitches. Therefore, the photoswitching systems with longer bridge lengths are better for improving storage energy due to *N*-substitution at the bridgehead and unsaturated position.

Since molecular photoswitching systems must have a low molecular weight, energy storage density is a more useful



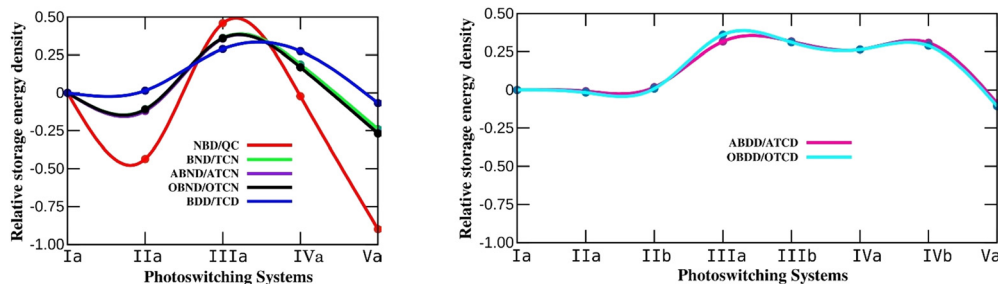


Fig. 3 Variation in the energy storage density of *N*-substituted systems relative to that of their parent photoswitching system. The energy values were obtained by computing the electronic energy with the DLPNO-CCSD(T)/Def2TZVP method and including thermal correction at the M062X/6-311++G\*\* level.

quantity to predict the properties of MOST systems. Therefore, energy storage density is calculated for all the studied systems and the values are tabulated in S2 of the ESI† (Tables S2–S8). The variation in energy storage density of *N*-substituted chemical photoswitches relative to the parent systems is depicted in Fig. 3. It is apparent from the figure that the energy storage density in aza-bicyclodiene based photoswitches depends on the position of *N*. The trend observed for the variation in energy storage density for the different *N*-substituted systems is similar to that of storage energy. Since aza-bicyclodiene photoswitches are isobaric with their parent system, the energy density is not affected due to the mass of *N*. The properties of photoswitching systems are usually tuned by substituting electron donating and withdrawing groups, which reduces the energy storage density.<sup>58</sup> In aza-bicyclodiene switches, *N* may internally involve a push-pull mechanism and the properties can be tuned without reducing the energy storage density due to the mass of *N*, and thus is advantageous over bulky group substituents.<sup>59</sup>

**Thermal back reaction barrier ( $\Delta E_{\text{TBR}}$ ).** A larger thermal back reaction barrier ( $\Delta E_{\text{TBR}}$ ) is essential to extend the lifespan of the metastable photoisomer and store solar energy as chemical energy for a longer period. Therefore, attention has also been devoted to estimating the energy required to convert the photoproduct to bicyclodiene in various *N*-substituted photoswitches. The calculated barrier height ( $\Delta E_{\text{TBR}}$ ) for the thermal back isomerization reaction of the studied photoswitching couples is provided in S2 of the ESI† (Tables S2–S8). The variation in  $\Delta E_{\text{TBR}}$  for different aza-bicyclodiene photoswitching

systems relative to that of their parent systems is displayed in Fig. 4. Here,  $\Delta E_{\text{TBR}}$  for the parent photoswitch was assumed to be zero and the energies for various aza-substituted photoswitches were calculated relative to that of the parent switch.

During the thermal back conversion of the photoproduct to bicyclodiene, dissociation of the two bonds occurs through an asynchronous mechanism.<sup>22</sup> Initially, a bond is cleaved, leading to the formation of singlet biradicals in the transition state (TS).<sup>22</sup> Owing to the multireference character of TS, the DFT functionals are inappropriate for predicting the TS and they overestimate the energy barrier.<sup>22</sup> Multiconfigurational methods, like CASSCF, are rather more suitable for an accurate prediction of the energy barrier.<sup>22</sup> As multiconfigurational calculations are computationally expensive, they cannot be routinely employed for simulations.<sup>16,22</sup> A previous benchmark study demonstrated that the electronic energy calculated by CASSCF methods for TS geometries obtained using the PBE functional determine  $\Delta E_{\text{TBR}}$  close to the experimental values at a cheaper computational cost.<sup>22</sup> Therefore, in the present investigation, the geometry of transition states is obtained through climbing image nudged elastic band (CI-NEB) calculations using the PBE functional. Subsequently, the electronic energy of the transition states and photoproducts were computed with a single point energy calculation at the (8,8)-CASPT2/6-311++G\*\* level of theory.

It is apparent from the figure that the energy barrier for the thermal back conversion reaction significantly alters due to *N*-Substitution. Consistent with the storage energy, the observed

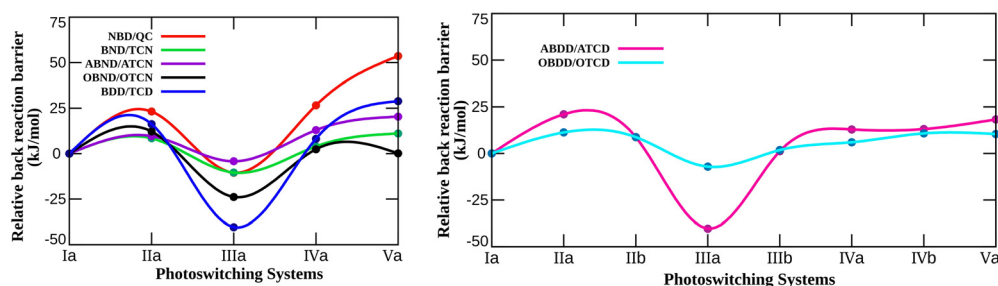


Fig. 4 Variation in the barrier for thermal back isomerization of the photoproduct to bicyclodiene in various *N*-substituted systems relative to that of their parent photoswitching system. The energy values were obtained by computing the electronic energy with the (8,8)-CASPT2/6-311++G\*\* level of theory.



trend for the thermal back reaction barrier in the aza-substituted photoswitches depends solely on the position of the N atom. As can be seen from the figure, the barrier height increases by 23.17 kJ mol<sup>-1</sup> when N is substituted at the bridgehead position (IIa-NBD/QC) in the NBD/QC photoswitching pair. If both the bridgehead positions are replaced with N atoms (Va-NBD/QC), a substantial increment (53.62 kJ mol<sup>-1</sup>) in the energy barrier is noticed. In contrast, if the unsaturated C is replaced with N (IIIa-NBD/QC), the  $\Delta E_{\text{TBR}}$  decreases by 10.52 kJ mol<sup>-1</sup>. Moreover, the barrier increases by 26.56 kJ mol<sup>-1</sup> when the bridgehead and nearest unsaturated C atoms are replaced with N (IVa-NBD/QC). This clearly indicates that the presence of N in the bridgehead position enhances the energy barrier for the thermal back conversion reaction. Further, substitution of N in the unsaturated position lowers the energy barrier relative to that of the parent photoswitching system. The trend observed for  $\Delta E_{\text{TBR}}$  in various *N*-substituted NBD/QC systems is opposite to that of  $\Delta G_{\text{str}}$  (Fig. 3 and 4). This simply means that when the thermal back reaction barrier for *N*-substitution in the short-bridged NBD/QC photoswitches is increased, then the storage energy is adversely affected and *vice versa*.

The variation in  $\Delta E_{\text{TBR}}$  with *N*-substitution in the photoswitches of different bridge length relative to that of their parent system follows the same trend as that of the aza-NBD/QC pair. Therefore,  $\Delta E_{\text{TBR}}$  also increases with the presence of N at the bridgehead position in the photoswitching systems with a longer bridge length. The calculated increase in the energy barriers of the thermal back reaction in the IIa-BDD/TCD and Va-BDD/TCD systems relative to that of their parent BDD/TCD pair are 16.28 and 28.88 kJ mol<sup>-1</sup>, respectively. As mentioned earlier, the reducing effect of  $\Delta G_{\text{str}}$  with bridgehead *N*-substitution becomes less prominent as the bridge length increases in bicyclodiene-based switches. Therefore, the *N*-substitution at the bridgehead position of the long-bridge photoswitching systems can uplift the barrier height ( $\Delta E_{\text{TBR}}$ ) without compromising the storage energy.

The overall analysis of thermochemical properties explicitly advocates that the presence of heteroatoms on the bridge have a minimal impact on the photoswitching properties, whereas replacement of the bridgehead or unsaturated C of bicyclodiene by N has a significant effect. Close analysis of the storage energy suggests that the substitution of N at one of the unsaturated C atoms in bicyclodiene remarkably improves the storage energy of the photoswitching system. The storage energy decreases when N is present at the bridgehead position in the short-bridge bicyclodiene photoswitch (NBD/QC pair). Interestingly, the decrease in storage energy becomes less prominent as the bridge length increases. Moreover, the barrier height for thermal back isomerization increases in bridgehead *N*-substituted systems. Thus, *N*-substitution at the bridgehead position of the long-bridge bicyclodiene photoswitch (aza-BDD/TCD) exhibits better thermochemical properties than those of the parent BDD/TCD pair. Therefore, it is interesting to mention that in the case of long-bridge photoswitches, the lifespan of the metastable photo-product can be enhanced without adversely affecting the amount of energy harnessed from solar radiation.

The short-bridged NBD/QC has the least storage energy (96.06 kJ mol<sup>-1</sup>) and highest TBR barrier (121.76 kJ mol<sup>-1</sup>). Contrarily, the long bridged BDD/TCD couple displays the largest storage energy (304.39 kJ mol<sup>-1</sup>) with the least thermal barrier (37.63 kJ mol<sup>-1</sup>). This clearly infers that an increase in bridge length enhances storage energy of the bicyclic diene photoswitches and compromises the TBR barrier, which is in accordance with the previous report.<sup>16</sup> Owing to the large storage energy of the long bridged BDD/TCD couple, it could be considered as a better system to further investigate in the future, as it provides a large scope for tuning the photoswitching properties. Therefore, any structural modifications in the long bridged bicyclic dienes that enhance the thermal barrier for isomerization are desirable for engineering the MOST system.

Outcomes of this work reveal that the impact of *N*-substitution in these bicyclic dienes depends upon the position of N and size of the bridge. *N*-substitution at one of the unsaturated positions in diene (III) increases the storage energy by 41.94–51.60 kJ mol<sup>-1</sup> at the expense of the TBR barrier. The *N*-substitution at the bridgehead position (II and III) enhances the barrier for thermal isomerization at the cost of storage energy in the case of short bridged photoswitches. In contrast to this, *N*-substitution at the bridgehead position enhances the barrier for thermal isomerization without compromising the storage energy in the case of long bridged photoswitches.

Overall, the impact of *N*-substitution at bridgehead position in the long bridged Va-BDD/TCD couple is the enhancement of TBR by 28.88 kJ mol<sup>-1</sup> without significantly reducing the energy storage density relative to that of the Ia-BDD/TCD pair. Therefore, the *N*-substitution assists tuning the properties of the studied bridged bicyclic diene photoswitches and may guide the future designing of photoswitches for practical MOST applications. Despite the highest increment in TBR, the absolute TBR barrier of IIa- and Va-BDD/TCD systems remains lower than that desired for long-time energy storage devices due to the low intrinsic barrier in the Ia-BDD/TCD system. The results suggest that *N*-substitution at the bridgehead position could be one of the approaches that will considerably enhance the thermal barrier, while further substitutions must be carried out to make it relevant for practical MOST applications.

Furthermore, the substitution of N at the bridgehead and closest unsaturated position (IV) increases the TBR barrier and storage energy. Therefore, the molecules with these *N*-substitutions display the best photoswitching properties among the studied switches for MOST applications. The intrinsic TBR barrier of the short-bridged NBD/QC system is larger, and *N*-substitutions enhance the TBR barrier to 148.33 kJ mol<sup>-1</sup> without compromising the storage energy. Thus, among the studied photochromic couples, IVa-NBD/QC could be considered as the best system for energy storage applications.

### 3.3 Photophysical properties

Absorption of solar radiation by the molecule is one of the prerequisites to serve as a photoswitching system for MOST applications. Therefore, critical analysis of the photophysical



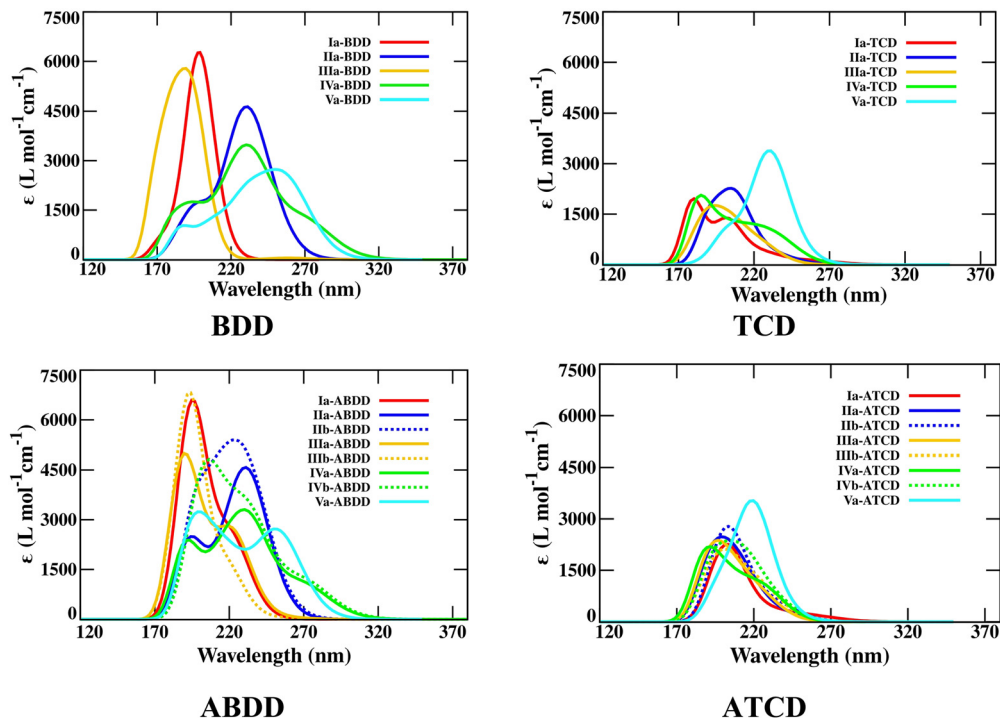


Fig. 5 Optical absorption spectra of the parent and *N*-substituted BDD/TCD and ABDD/ATCD photoswitching systems.

properties of the photoswitching couple is important. The photophysical properties of the studied photochromic couples were calculated and the optical absorption spectra of the parent BDD/TCD, ABDD/ATCD, their various *N*-substituted bicyclobutadienes and corresponding photoproducts are depicted in Fig. 5. The optical spectra of other studied systems are provided in S3 of the ESI† (Fig. S1). The spectral data, including the molar absorption coefficient, first important excitation wavelength and oscillatory strength (surpassing 0.01), are tabulated in S3 of ESI† (Tables S9–S15).

The calculated first excitation wavelengths for NBD, BND, and BDD are 214.42, 206.69, and 207.52 nm, respectively, which is in close agreement with the recently reported values of 213.65, 206.67, and 207.66 nm.<sup>16</sup> The photophysical properties are greatly influenced by the substitution of *N* in these bicyclobutadienes. Further, the optical absorption spectra (optical properties) vary with the position of *N* in bicyclobutadiene molecules similar to that of thermochemical properties. It is noteworthy that the presence of *N* at the bridgehead position considerably red-shifts the first important excitation wavelength of bicyclobutadienes. The red-shift in the excitation wavelength becomes more prominent when both bridgehead C atoms are replaced with *N*. It has been noticed that the replacement of unsaturated C with *N* in bicyclobutadienes shows a slight hypsochromic shift in the first important excitation wavelength. This demonstrates that the position of *N* plays a crucial role in modulating the photophysical properties of bicyclobutadiene-based photoswitching systems, analogous with the thermochemical properties.

Upon substitution of both the bridgehead C atoms with *N*, bathochromic shifts of 58.67 and 51.63 nm are noticed in the

first excitation wavelengths of Va-BND and Va-BDD, respectively, when compared with those of their parent molecules. The first optical excitation wavelength of Va-BDD is 271.66 nm which is longer than the first excitation wavelength of the most studied NBD (213.65 nm), recently reported bicyclooctadiene (196.44 nm), and unsubstituted bicyclobutadiene molecules with different bridge lengths.<sup>16</sup>

*En route* to probe the delocalization of electrons in aza-bicyclobutadiene based photoswitches, natural bond orbital (NBO) analyses have been performed for the bicyclic diene and photoproducts. It has been observed that the lone pair of bridgehead *N* ( $N_{lp}$ ) involves the delocalization with  $\pi^*$ -bonding orbitals in the bicyclic diene. The stabilization energy for the  $N_{lp} \rightarrow \pi^*$  charge transfer is 1.21, 3.25, and 15.13 kcal mol<sup>-1</sup> in the IIa-NBD, IIa-BND, and IIa-BDD molecules, respectively. This infers that the extent of stabilization achieved due to  $N_{lp} \rightarrow \pi^*$  electron delocalization increases with the length of the bridge. Likewise, the extent of stabilization achieved due to the  $N_{lp} \rightarrow \sigma^*$  charge transfer in the photoproduct increases from 4.88 kcal mol<sup>-1</sup> in IIa-QC to 14.33 kcal mol<sup>-1</sup> in IIa-TCD. This suggests that the lone pair on *N* may involve an internal push-pull mechanism and assist to modulate the properties of the photoswitches. The stabilization achieved due to the delocalization of  $N_{lp}$  to  $\pi^*$ -bonding orbitals in bridgehead *N*-substituted (II) bicyclic diene photoswitches of different bridge lengths is shown in Fig. 6. In contrast to the bridgehead *N*, the lone pair on unsaturated *N* does not facilitate delocalization with the  $\pi^*$ -bonding orbitals.

The relationship of the molecular structure, particularly the position of *N* with the thermochemical and photophysical properties is systematically summarized in a concise manner





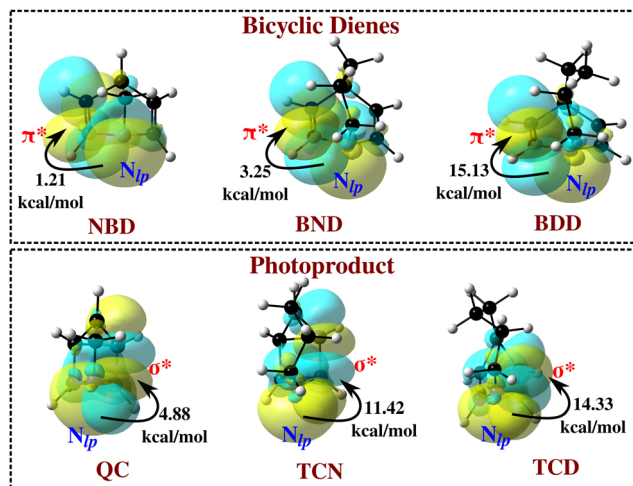


Fig. 6 The stabilization achieved due to delocalization of  $N_{lp}$  in bridgehead  $N$ -substituted bicyclic diene photoswitches with different bridge lengths.

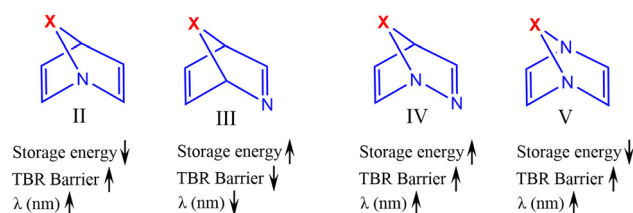


Fig. 7 Systematic summary of the relationships of the molecular structure, particularly the position of N with the thermochemical and photophysical properties.

in Fig. 7. The results reveal that the substitution of N at the bridgehead position (II) increases the TBR barrier and the first important wavelength of excitation at the cost of the storage energy. The effect is found to be more pronounced if both the bridgehead positions are substituted with N (V). In contrast, the presence of N at the unsaturated position (III) improves the storage energy while the TBR barrier and wavelength of absorption is observed to decrease. Further, the substitution of N at the bridgehead and the closest unsaturated position (IV) mostly increases all three parameters in the studied bridged bicyclic diene photoswitches.

## 4. Conclusion

The decreasing ring strain energy (28.95 to 4.28 kcal mol<sup>-1</sup>) stabilizes the bicyclodiene, whereas increasing ring SE (89.75 to 115.19 kcal mol<sup>-1</sup>) destabilizes the metastable photoproduct with progressive increase in bridge length of the bicyclodiene-based photoswitches. Therefore, the storage energy is improved while the barrier for the thermal back reaction is reduced with an increase in  $-CH_2-$  units in the bridge. The photoswitching properties of the bridged bicyclodiene-based photoswitches can be significantly altered with the  $N$ -substitution and are

governed by the position of N. The thermochemical properties elucidate that the replacement of unsaturated C in bicyclodiene with N increases the storage energy but decreases the thermal back reaction barrier. The presence of N at the bridgehead position in the NBD/QC increases the barrier for thermal isomerization at the cost of storage energy. The decrease in storage energy due to  $N$ -substitution at the bridgehead position becomes less prominent with an increase in bridge length. Therefore, it is worth mentioning that the thermal back reaction barrier of the bridgehead  $N$ -substituted BDD/TCD photo-switch can be uplifted by 28.88 kJ mol<sup>-1</sup> without compromising storage energy. Furthermore, the replacement of bridgehead C with N remarkably red-shifts the first important excitation wavelength. Therefore,  $N$ -substitution significantly improves the thermochemical and photophysical properties, particularly of the long-bridged bicyclic diene switches. Moreover, the substitution of N at the bridgehead and the closest unsaturated position improves the storage energy, TBR barrier and first excitation wavelength of the studied photoswitching pairs, making them more relevant for MOST applications. The outcomes exclusively emphasize that the  $N$ -substitution can greatly modulate the photoswitching properties and will, indeed, be beneficial for future designing of a novel photochromic couple for practical MOST applications.

## Conflicts of interest

The authors declare there are no conflicts of interest.

## Acknowledgements

We are sincerely thankful to the DST-SERB (EEQ/2023/000424, ECR/2018/002346 and EEQ/2019/000656) for providing the financial support for this work. We are grateful to the Director, National Institute of Technology Warangal (NITW), Warangal, for providing all the facilities required for this work. AAS wishes to thank SERB for the JRF and SERB and the Ministry of Education (MoE), India, for the SRF, and RKK wishes to thank the MoE, India, for the SRF.

## References

- P. J. Megía, A. J. Vizcaíno, J. A. Calles and A. Carrero, Hydrogen Production Technologies: From Fossil Fuels toward Renewable Sources. A Mini Review, *Energy Fuels*, 2021, **35**, 16403–16415.
- N. S. Lewis and D. G. Nocera, Powering the planet: Chemical challenges in solar energy utilization, *Proc. Natl. Acad. Sci. U. S. A.*, 2006, **103**, 15729–15735.
- C. Ngô and J. B. Natowitz, *Our Energy Future*, John Wiley & Sons, Ltd, 2016, pp. 1–25.
- M. Grätzel, Powering the planet, *Nature*, 2000, **403**, 363.
- J. Orrego-Hernández, A. Dreos and K. Moth-Poulsen, Engineering of Norbornadiene/Quadricyclane Photoswitches for



- Molecular Solar Thermal Energy Storage Applications, *Acc. Chem. Res.*, 2020, **53**, 1478–1487.
- 6 J. S. Amthor, From sunlight to phytomass: on the potential efficiency of converting solar radiation to phyto-energy, *New Phytol.*, 2010, **188**, 939–959.
  - 7 E. Collini, Light-Harvesting: The Never-Ending Lesson of Nature, *ACS Cent. Sci.*, 2022, **8**, 306–308.
  - 8 G. D. Scholes, G. R. Fleming, A. Olaya-Castro and R. van Grondelle, Lessons from nature about solar light harvesting, *Nat. Chem.*, 2011, **3**, 763–774.
  - 9 J. Su and L. Vayssieres, A Place in the Sun for Artificial Photosynthesis?, *ACS Energy Lett.*, 2016, **1**, 121–135.
  - 10 D. K. Dogutan and D. G. Nocera, Artificial Photosynthesis at Efficiencies Greatly Exceeding That of Natural Photosynthesis, *Acc. Chem. Res.*, 2019, **52**, 3143–3148.
  - 11 Y. Gao, K. Huang, C. Long, Y. Ding, J. Chang, D. Zhang, L. Etgar, M. Liu, J. Zhang and J. Yang, Flexible Perovskite Solar Cells: From Materials and Device Architectures to Applications, *ACS Energy Lett.*, 2022, **7**, 1412–1445.
  - 12 M. Melchionna and P. Fornasiero, Updates on the Roadmap for Photocatalysis, *ACS Catal.*, 2020, **10**, 5493–5501.
  - 13 V. Romano, G. D'Angelo, S. Perathoner and G. Centi, Current density in solar fuel technologies, *Energy Environ. Sci.*, 2021, **14**, 5760–5787.
  - 14 Z. Wang, H. Hölzel and K. Moth-Poulsen, Status and challenges for molecular solar thermal energy storage system based devices, *Chem. Soc. Rev.*, 2022, **51**, 7313–7326.
  - 15 M.-M. Russew and S. Hecht, Photoswitches: From Molecules to Materials, *Adv. Mater.*, 2010, **22**, 3348–3360.
  - 16 A. E. Hillers-Bendtsen, P. G. Iuel Lunøe Dünweber, L. H. Olsen and K. V. Mikkelsen, Prospects of Improving Molecular Solar Energy Storage of the Norbornadiene/Quadricyclane System through Bridgehead Modifications, *J. Phys. Chem. A*, 2022, **126**, 2670–2676.
  - 17 A. E. Hillers-Bendtsen, M. Quant, K. Moth-Poulsen and K. V. Mikkelsen, Investigation of the Structural and Thermochemical Properties of [2.2.2]-Bicyclooctadiene Photoswitches, *J. Phys. Chem. A*, 2021, **125**, 10330–10339.
  - 18 M. Quant, A. E. Hillers-Bendtsen, S. Ghasemi, M. Erdelyi, Z. Wang, L. M. Muhammad, N. Kann, K. V. Mikkelsen and K. Moth-Poulsen, Synthesis, characterization and computational evaluation of bicyclooctadienes towards molecular solar thermal energy storage, *Chem. Sci.*, 2022, **13**, 834–841.
  - 19 A. Lennartson, A. Roffey and K. Moth-Poulsen, Designing photoswitches for molecular solar thermal energy storage, *Tetrahedron Lett.*, 2015, **56**, 1457–1465.
  - 20 M. Morikawa, Y. Yamanaka and N. Kimizuka, Liquid Bisazobenzenes as Molecular Solar Thermal Fuel with Enhanced Energy Density, *Chem. Lett.*, 2022, **51**, 402–406.
  - 21 Z. Wang, P. Erhart, T. Li, Z.-Y. Zhang, D. Sampedro, Z. Hu, H. A. Wegner, O. Brummel, J. Libuda, M. B. Nielsen and K. Moth-Poulsen, Storing energy with molecular photoisomers, *Joule*, 2021, **5**, 3116–3136.
  - 22 M. J. Kuisma, A. M. Lundin, K. Moth-Poulsen, P. Hyldgaard and P. Erhart, Comparative Ab-Initio Study of Substituted Norbornadiene-Quadricyclane Compounds for Solar Thermal Storage, *J. Phys. Chem. C*, 2016, **120**, 3635–3645.
  - 23 E. N. Cho, D. Zhitomirsky, G. G. D. Han, Y. Liu and J. C. Grossman, Molecularly Engineered Azobenzene Derivatives for High Energy Density Solid-State Solar Thermal Fuels, *ACS Appl. Mater. Interfaces*, 2017, **9**, 8679–8687.
  - 24 Z. Yoshida, New molecular energy storage systems, *J. Photochem.*, 1985, **29**, 27–40.
  - 25 V. A. Bren', A. D. Dubonosov, V. I. Minkin and V. A. Chernovyanov, Norbornadiene–quadricyclane—an effective molecular system for the storage of solar energy, *Russ. Chem. Rev.*, 1991, **60**, 451.
  - 26 A. D. Dubonosov, V. A. Bren and V. A. Chernovyanov, Norbornadiene–quadricyclane as an abiotic system for the storage of solar energy, *Russ. Chem. Rev.*, 2002, **71**, 917.
  - 27 M. Bertram, F. Waidhas, M. Jevric, L. Fromm, C. Schuschke, M. Kastenmeier, A. Görling, K. Moth-Poulsen, O. Brummel and J. Libuda, Norbornadiene photoswitches anchored to well-defined oxide surfaces: From ultrahigh vacuum into the liquid and the electrochemical environment, *J. Chem. Phys.*, 2020, **152**, 044708.
  - 28 K. Börjesson, A. Lennartson and K. Moth-Poulsen, Efficiency Limit of Molecular Solar Thermal Energy Collecting Devices, *ACS Sustainable Chem. Eng.*, 2013, **1**, 585–590.
  - 29 K. Börjesson, A. Lennartson and K. Moth-Poulsen, Fluorinated fulvalene ruthenium compound for molecular solar thermal applications, *J. Fluorine Chem.*, 2014, **161**, 24–28.
  - 30 U. Jacovella, E. Carrascosa, J. T. Buntine, N. Ree, K. V. Mikkelsen, M. Jevric, K. Moth-Poulsen and E. J. Bieske, Photo- and Collision-Induced Isomerization of a Charge-Tagged Norbornadiene–Quadricyclane System, *J. Phys. Chem. Lett.*, 2020, **11**, 6045–6050.
  - 31 F. Waidhas, M. Jevric, M. Bosch, T. Yang, E. Franz, Z. Liu, J. Bachmann, K. Moth-Poulsen, O. Brummel and J. Libuda, Electrochemically controlled energy release from a norbornadiene-based solar thermal fuel: increasing the reversibility to 99.8% using HOPG as the electrode material, *J. Mater. Chem. A*, 2020, **8**, 15658–15664.
  - 32 Z. Wang, H. Hölzel and K. Moth-Poulsen, Status and challenges for molecular solar thermal energy storage system based devices, *Chem. Soc. Rev.*, 2022, **51**, 7313–7326.
  - 33 Z. Wang, H. Moïse, M. Cacciarini, M. B. Nielsen, M. Morikawa, N. Kimizuka and K. Moth-Poulsen, Liquid-Based Multijunction Molecular Solar Thermal Energy Collection Device, *Adv. Sci.*, 2021, **8**, 2103060.
  - 34 Z. Wang, Z. Wu, Z. Hu, J. Orrego-Hernández, E. Mu, Z.-Y. Zhang, M. Jevric, Y. Liu, X. Fu, F. Wang, T. Li and K. Moth-Poulsen, Chip-scale solar thermal electrical power generation, *Cell Rep. Phys. Sci.*, 2022, **3**, 100789.
  - 35 A. Kjaersgaard, H. Hölzel, K. Moth-Poulsen and M. B. Nielsen, Photolytic Studies of Norbornadiene Derivatives under High-Intensity Light Conditions, *J. Phys. Chem. A*, 2022, **126**, 6849–6857.
  - 36 A. E. Hillers-Bendtsen, M. H. Hansen and K. V. Mikkelsen, The influence of nanoparticles on the excitation energies of



- the photochromic dihydroazulene/vinylheptafulvene system, *Phys. Chem. Chem. Phys.*, 2019, **21**, 6689–6698.
- 37 A. E. Hillers-Bendtsen, M. B. Johansen and K. V. Mikkelsen, Promoting the thermal back reaction of vinylheptafulvene to dihydroazulene by physisorption on nanoparticles, *Phys. Chem. Chem. Phys.*, 2021, **23**, 12889–12899.
- 38 S. Helmy, F. A. Leibfarth, S. Oh, J. E. Poelma, C. J. Hawker and J. Read de Alaniz, Photoswitching Using Visible Light: A New Class of Organic Photochromic Molecules, *J. Am. Chem. Soc.*, 2014, **136**, 8169–8172.
- 39 S. Crespi, N. A. Simeth and B. König, Heteroaryl azo dyes as molecular photoswitches, *Nat. Rev. Chem.*, 2019, **3**, 133–146.
- 40 P. Bolle, C. Menet, M. Puget, H. Serier-Brault, S. Katao, V. Guerchais, F. Boucher, T. Kawai, J. Boixel and R. Dessapt, Enhanced reversible solid-state photoswitching of a cationic dithienylethene assembled with a polyoxometalate unit, *J. Mater. Chem. C*, 2021, **9**, 13072–13076.
- 41 R. Eschenbacher, T. Xu, E. Franz, R. Löw, T. Moje, L. Fromm, A. Görling, O. Brummel, R. Herges and J. Libuda, Triggering the energy release in molecular solar thermal systems: Norbornadiene-functionalized trioxatriangulen on Au(111), *Nano Energy*, 2022, **95**, 107007.
- 42 G. Li, L. Sun, L. Ji and H. Chao, Ruthenium(II) complexes with dppz: from molecular photoswitch to biological applications, *Dalton Trans.*, 2016, **45**, 13261–13276.
- 43 R. Boese, J. K. Cammack, A. J. Matzger, K. Pflug, W. B. Tolman, K. P. C. Vollhardt and T. W. Weidman, Photochemistry of (Fulvalene)tetracarbonyldiruthenium and Its Derivatives: Efficient Light Energy Storage Devices, *J. Am. Chem. Soc.*, 1997, **119**, 6757–6773.
- 44 A. A. Beharry and G. A. Woolley, Azobenzene photoswitches for biomolecules, *Chem. Soc. Rev.*, 2011, **40**, 4422–4437.
- 45 M. W. H. Hoorens, M. Medved', A. D. Laurent, M. Di Donato, S. Fanetti, L. Slappendel, M. Hilbers, B. L. Feringa, W. Jan Buma and W. Szymanski, Iminothioindoxyl as a molecular photoswitch with 100 nm band separation in the visible range, *Nat. Commun.*, 2019, **10**, 2390.
- 46 J. L. Greenfield, M. A. Gerkman, R. S. L. Gibson, G. G. D. Han and M. J. Fuchter, Efficient Electrocatalytic Switching of Azoheteroarenes in the Condensed Phases, *J. Am. Chem. Soc.*, 2021, **143**, 15250–15257.
- 47 R. Zhao, Y. Li, J. Bai, J. Mu, L. Chen, N. Zhang, J. Han, F. Liu and S. Yan, Preparation of flexible photo-responsive film based on novel photo-liquefiable azobenzene derivative for solar thermal fuel application, *Dyes Pigm.*, 2022, **202**, 110277.
- 48 M. Cacciarini, M. Jevric, J. Elm, A. U. Petersen, K. V. Mikkelsen and M. B. Nielsen, Fine-tuning the lifetimes and energy storage capacities of meta-stable vinylheptafulvenes via substitution at the vinyl position, *RSC Adv.*, 2016, **6**, 49003–49010.
- 49 M. D. Kilde, P. G. Arroyo, A. S. Gertsen, K. V. Mikkelsen and M. B. Nielsen, Molecular solar thermal systems – control of light harvesting and energy storage by protonation/deprotonation, *RSC Adv.*, 2018, **8**, 6356–6364.
- 50 A. Mengots, A. Erbs Hillers-Bendtsen, S. Doria, F. Ørsted Kjeldal, N. Machholdt Høyer, A. Ugleholdt Petersen, K. V. Mikkelsen, M. Di Donato, M. Cacciarini and M. Brøndsted Nielsen, Dihydroazulene-Azobenzene-Dihydroazulene Triad Photoswitches, *Chem. – Eur. J.*, 2021, **27**, 12437–12446.
- 51 M. H. Cardenuto, H. M. Cezar, K. V. Mikkelsen, S. P. A. Sauer, K. Coutinho and S. Canuto, A QM/MM study of the conformation stability and electronic structure of the photochromic switches derivatives of DHA/VHF in acetonitrile solution, *Spectrochim. Acta, Part A*, 2021, **251**, 119434.
- 52 R. Asato, C. J. Martin, T. Nakashima, J. P. Calupitan, G. Rapenne and T. Kawai, Energy Storage upon Photochromic 6- $\pi$  Photocyclization and Efficient On-Demand Heat Release with Oxidation Stimuli, *J. Phys. Chem. Lett.*, 2021, **12**, 11391–11398.
- 53 G. Jones, T. E. Reinhardt and W. R. Bergmark, Photon energy storage in organic materials—The case of linked anthracenes, *Sol. Energy*, 1978, **20**, 241–248.
- 54 P. Lorenz, F. Wullschläger, A. Rüter, B. Meyer and A. Hirsch, Tunable Photoswitching in Norbornadiene (NBD)/Quadricyclane (QC) – Fullerene Hybrids, *Chem. – Eur. J.*, 2021, **27**, 14501–14507.
- 55 N. Ree and K. V. Mikkelsen, Benchmark study on the optical and thermochemical properties of the norbornadiene-quadricyclane photoswitch, *Chem. Phys. Lett.*, 2021, **779**, 138665.
- 56 A. E. Hillers-Bendtsen, F. Ø. Kjeldal, N. M. Høyer and K. V. Mikkelsen, Optimization of the thermochemical properties of the norbornadiene/quadricyclane photochromic couple for solar energy storage using nanoparticles, *Phys. Chem. Chem. Phys.*, 2022, **24**, 5506–5521.
- 57 R. Szabo, K. N. Le and T. Kowalczyk, Multifactor theoretical modeling of solar thermal fuels built on azobenzene and norbornadiene scaffolds, *Sustainable Energy Fuels*, 2021, **5**, 2335–2346.
- 58 A. E. Hillers-Bendtsen, J. L. Elholm, O. B. Obel, H. Hölzel, K. Moth-Poulsen and K. V. Mikkelsen, Searching the Chemical Space of Bicyclic Dienes for Molecular Solar Thermal Energy Storage Candidates, *Angew. Chem.*, 2023, e202309543.
- 59 A. A. Sangolkar, M. Faizan, K. R. Krishna and R. Pawar, Azabicyclooctadiene/tetracyclooctane couples as promising photoswitches for molecular solar thermal energy storage applications, *Mol. Syst. Des. Eng.*, 2023, **8**, 853–865.
- 60 P. R. Rablen, A Procedure for Computing Hydrocarbon Strain Energies Using Computational Group Equivalents, with Application to 66 Molecules, *Chemistry*, 2020, **2**, 347–360.
- 61 M. J. Frisch, G. W. Trucks, H. B. Schlegel, G. E. Scuseria, M. A. Robb, J. R. Cheeseman, G. Scalmani, V. Barone, G. A. Petersson, H. Nakatsuji, X. Li, M. Caricato, A. V. Marenich, J. Bloino, B. G. Janesko, R. Gomperts, B. Mennucci, H. P. Hratchian, J. V. Ortiz, A. F. Izmaylov, J. L. Sonnenberg, D. Williams-Young, F. Ding, F. Lipparini, F. Egidi, J. Goings, B. Peng, A. Petrone, T. Henderson, D. Ranasinghe, V. G. Zakrzewski, J. Gao, N. Rega, G. Zheng, W. Liang, M. Hada, M. Ehara, K. Toyota, R. Fukuda, J. Hasegawa, M. Ishida, T. Nakajima, Y. Honda, O. Kitao, H. Nakai,



- T. Vreven, K. Throssell, J. A. Montgomery Jr., J. E. Peralta, F. Ogliaro, M. J. Bearpark, J. J. Heyd, E. N. Brothers, K. N. Kudin, V. N. Staroverov, T. A. Keith, R. Kobayashi, J. Normand, K. Raghavachari, A. P. Rendell, J. C. Burant, S. S. Iyengar, J. Tomasi, M. Cossi, J. M. Millam, M. Klene, C. Adamo, R. Cammi, J. W. Ochterski, R. L. Martin, K. Morokuma, O. Farkas, J. B. Foresman and D. J. Fox, *Gaussian 16, Revision C.01*, 2016.
- 62 P. Giannozzi, O. Barone, P. Bonfà, D. Brunato, R. Car, I. Carnimeo, C. Cavazzoni, S. de Gironcoli, P. Delugas, F. Ferrari Ruffino, A. Ferretti, N. Marzari, I. Timrov, A. Urru and S. Baroni, Quantum ESPRESSO toward the exascale, *J. Chem. Phys.*, 2020, **152**, 154105.
- 63 F. Neese, Software update: the ORCA program system, version 4.0, *Wiley Interdiscip. Rev.: Comput. Mol. Sci.*, 2018, **8**, e1327.
- 64 X. An and Y. Xie, Enthalpy of isomerization of quadricyclane to norbornadiene, *Thermochim. Acta*, 1993, **220**, 17–25.
- 65 V. Gray, A. Lennartson, P. Ratanalert, K. Börjesson and K. Moth-Poulsen, Diaryl-substituted norbornadienes with red-shifted absorption for molecular solar thermal energy storage, *Chem. Commun.*, 2014, **50**, 5330–5332.
- 66 E. Vessally, Maximizing the Solar Energy Storage of the Norbornadiene-Quadricyclane System: Mono-Heteroatom Effect by DFT Calculations, *Phosphorus, Sulfur Silicon Relat. Elem.*, 2009, **184**, 2307–2313.

